ARTICLE
Journal of Cellular Biochemistry 113:1692–1703 (2012)

Journal of Cellular Biochemistry

Phosphofructokinase Type 1 Kinetics, Isoform Expression, and Gene Polymorphisms in Cancer Cells

Rafael Moreno-Sánchez,* Alvaro Marín-Hernández, Juan Carlos Gallardo-Pérez, Héctor Quezada, Rusely Encalada, Sara Rodríguez-Enríquez, and Emma Saavedra

Departamento de Bioquímica, Instituto Nacional de Cardiología, México D.F. 14080, Mexico

ABSTRACT

Kinetic analysis of PFK-1 from rodent AS-30D, and human HeLa and MCF-7 carcinomas revealed sigmoidal [fructose 6-phosphate, Fru6P]-rate curves with different V_m values when varying the allosteric activator fructose 2,6 bisphosphate (Fru2,6BP), AMP, Pi, NH_4^+, or K^+. The rate equation that accurately predicted this behavior was the exclusive ligand binding concerted transition model together with non-essential hyperbolic activation. PFK-1 from rat liver and heart also exhibited the mixed cooperative-hyperbolic kinetic behavior regarding activators. Lowering pH induced decreased affinity for Fru6P, Fru2,6BP, citrate, and ATP (as inhibitor); as well as decreased V_m and increased content of inactive (T) enzyme forms. High K^+ prompted increased (Fru6P) or decreased (activators) affinities; increased V_m; and increased content of active (R) enzyme forms. mRNA expression analysis and nucleotide sequencing showed that the three PFK-1 isoforms L, M, and C are transcribed in the three carcinomas. However, proteomic analysis indicated the predominant expression of L in liver, of M in heart and MCF-7 cells, of L > M in AS-30D cells, and of C in HeLa cells. PFK-1M showed the highest affinities for F6P and citrate and the lowest for ATP (substrate) and F2,6BP; PFK-1L showed the lowest affinity for F6P and the highest for F2,6BP; and PFK-1C exhibited the highest affinity for ATP (substrate) and the lowest for citrate. Thus, the present work documents the kinetic signature of each PFK-1 isoform, and facilitates the understanding of why this enzyme exerts significant or negligible glycolysis flux-control in normal or cancer cells, respectively, and how it regulates the onset of the Pasteur effect. J. Cell. Biochem. 113: 1692–1703, 2012.

KEY WORDS: COOPERATIVE CONCERTED TRANSITION KINETIC MODEL; NON-ESSENTIAL HYPERBOLIC ACTIVATION; TUMOR GLYCOLYSIS; PASTEUR EFFECT

The control of the glycolytic flux, and hence the rate of ATP synthesis in the cytosol, is shared mainly by hexokinase (HK), ATP–phosphofructokinase type 1 (PFK-1), and glucose transporter (GLUT) in normal, healthy cells such as erythrocytes, hepatocytes, skeletal muscle, and intact heart [Rapoport et al., 1974; Torres et al., 1986; Kashiwaya et al., 1994; Jannaschk et al., 1999]. On the other hand, all the glycolytic enzymes and transporters are over-expressed in cancer cells (reviewed in Moreno-Sánchez et al., 2007, 2009; Marín-Hernández et al., 2009), with HK and PFK-1 showing the highest overexpression in human breast carcinomas and leukemia and in experimental tumors [Vora et al., 1985a; El-Bacha et al., 2003; dos Santos et al., 2004; Marín-Hernández et al., 2009]. An increase in the content and activity of controlling steps induces an increased pathway flux, bringing about a decrease in their flux-control capacities, and leading to a re-distribution of the entire pathway control. Indeed, the flux-control exerted by PFK-1 in the glycolytic pathways of ascites AS-30D and cervix HeLa carcinomas is negligible [Marín-Hernández et al., 2006, 2011].

In mammalian cells, PFK-1 is a homo- or hetero-tetramer of L, M, and C (or P) isoforms. The main isoform expressed in liver and kidney is PFK-1L, whereas skeletal muscle has only PFK-1M; PFK-1C is predominantly expressed in platelets and placenta. A mixture of the three isoforms is found in all other tissues [Koster et al., 1980; reviewed in Marín-Hernández et al., 2009]. On the other hand, in some malignant human and rat tumor types and cancer cell lines, C or L, or both isoforms prevail over the M isoform [Oskam et al., 1985;

Abbreviations: Fru6P, fructose 6-phosphate; Fru2,6BP, fructose 2,6 bisphosphate; G6PDH, glucose-6-phosphate dehydrogenase; GLUT, glucose transporter; HK, hexokinase; HPI, hexose-phosphate isomerase; LDH, lactate dehydrogenase; PFK-1, phosphofructokinase type 1.

Additional Supporting Information may be found in the online version of this article.

Grant sponsor: CONACyT-México; Grant numbers: 80534, 123636, 83084, 106583, 107183; Grant sponsor: Instituto de Ciencia y Tecnología del Distrito Federal; Grant number: PICS08-5.

*Correspondence to: Rafael Moreno-Sánchez, PhD, Departamento de Bioquímica, Instituto Nacional de Cardiología, Juan Badiano No. 1, Seccion XVI, Tlalpan, Mexico D.F. 14080, Mexico. E-mail: rafael.moreno@cardiologia.org.mx

Received 15 December 2011; Accepted 15 December 2011 • DOI 10.1002/jcb.24039 • © 2011 Wiley Periodicals, Inc.
Published online 28 December 2011 in Wiley Online Library (wileyonlinelibrary.com).

Vora et al., 1985a; Sánchez-Martínez and Aragón, 1997], whereas, in human gliomas [Staal et al., 1987], the expression of both L and M isoforms increases, and in MOLT-4 leukemia and cervico-uterine HeLa and KB carcinomas the C subunit predominates [Vora et al., 1985a].

Each PFK-1 isoform seems to have different kinetic properties [Oskam et al., 1985; Vora et al., 1985b; Staal et al., 1987; Dunaway et al., 1988]. PFK-1M shows the highest affinity for F6P ($K_{0.5} = 0.6$–2 mM), it is the most sensitive to F2,6BP activation and the least sensitive to ATP as inhibitor. PFK-1L is the least sensitive isoform to inhibition by citrate ($IC_{50} = 0.18$ mM). PFK-1C has the lowest affinity for F6P ($K_{0.5} = 1.4$–4 mM) and it is more sensitive to citrate inhibition ($IC_{50} = 0.08$ mM). PFK-1 in cancer cells also seems to have slightly different kinetic properties [Meldolesi et al., 1976; Oskam et al., 1985; Colomer et al., 1987; Staal et al., 1987; Sánchez-Martínez et al., 2000]. PFK-1 from rat thyroid carcinoma and human leukemia and gliomas is more sensitive to F2,6BP activation and less sensitive to inhibition by ATP and citrate than PFK-1 from normal cells. In consequence, the PFK-1 kinetic and regulatory properties are determined by its composition regarding type and proportion of the different subunits within the cell. However, it is worth noting that in these previous studies on PFK-1 kinetics, the simple Hill equation has been used to analyze the experimental data in which half-maximal ligand concentrations ($K_{0.5}$, IC_{50}, A_{50}) are calculated; accordingly all of these kinetic constant values are highly dependent on the experimental conditions and, hence, very variable. Therefore, the Hill equation does not provide the proper quantitative affinity parameters such as K_m, K_i, and K_A for cooperative binding ligands.

To increase the glycolytic flux (and thus increase the cytosolic ATP synthesis) cancer cells predominantly over-express the controlling steps, such as PFK-1 isoforms, which may have diminished sensitivity to feed-back inhibition by ATP and citrate and increased sensitivity to activators. However, the role for activators such as F2,6BP and AMP in increasing PFK-1 activity (and pathway flux) is currently unclear because, detailed kinetic studies on PFK-1 are scarce. In addition, to accurately predict a physiologically significant increased PFK-1 activity, intracellular concentrations of its specific activators and inhibitors, as well as the K_A and K_i values (activation and inhibition constants, respectively), and the appropriate rate equation, are also required. Thus, a systematic kinetic analysis of tumor AS-30D, HeLa and MCF-7 PFK-1 activities was undertaken in the present study in regard to its substrates [fructose 6-phosphate (Fru6P), ATP], activators [fructose 2,6 bisphosphate (Fru2,6BP), AMP, Pi, NH_4^+, K^+], and inhibitors (ATP, citrate, H^+). For comparison, rat liver and heart PFK-1 activities were also analyzed.

MATERIALS AND METHODS

CHEMICALS

Lyophilized aldolase, α-glycerophosphate dehydrogenase, and triosephosphate isomerase, as well as Fru6P, NAD^+, NADH, $NADP^+$, , ATP, ADP, AMP, Fru2,6BP, citrate, EDTA, EGTA, dithiothreitol (DTT), phenylmethanesulfonyl fluoride (PMSF), MOPS, imidazole, and HEPES were from Sigma Chemical (St. Louis, MO). Ammonium sulfate suspensions of HK, glucose-6-phosphate dehydrogenase (G6PDH), citrate lyase, malate dehydrogenase, and lactate dehydrogenase (LDH) were from Roche (Manheim, Germany). Recombinant pyruvate phosphate dikinase (PPDK) from *Entamoeba histolytica* was prepared as previously described [Saavedra et al., 2005]. All other reagents were of analytical grade.

CULTURE OF TUMOR CELLS

AS-30D hepatoma cells were propagated in female Wistar rats by intra-peritoneal injection and isolated as described elsewhere [López-Gómez et al., 1993]. Human carcinomas (cervico-uterine HeLa; epithelial breast MCF-7 and MDA-MB-231; prostate PC3; colon HCT15; non-small cell lung A549 and SKLU; brain U87MG) as well as rat glioma C6 were grown in Dulbecco's minimal essential medium (Gibco Life Technologies, Rockville, MD), supplemented with 10% fetal bovine serum (Gibco) and streptomycin/penicillin in 150-cm^2 Petri dishes (Corning, New York, NY) at 37°C in 5% CO_2/95% air.

CYTOSOLIC CELL FRACTIONS FROM TUMOR CELLS AND RAT LIVER AND HEART

AS-30D hepatoma cells were collected from the rat ascites fluid 5–7 days after inoculation. HeLa cells were harvested from 75% to 90% confluent cultures. Cells were re-suspended in 25 mM Tris/HCl buffer, pH 7.6, with 1 mM EDTA, 5 mM DTT, and 1 mM PMSF at a concentration of 65 mg protein/ml. The cell suspension was frozen in liquid nitrogen and thawed in a water bath at 37°C; this procedure was repeated three times. Cell lysates were centrifuged at 39,000*g* for 20 min at 4°C. The supernatant (i.e., the cytosolic-enriched fraction) was collected, mixed with 10% (v/v) glycerol and stored at −72°C until use for determination of enzyme activity. Under these conditions, PFK-1 activity remained constant for several weeks.

Liver and heart from 250 to 300 g female Wistar rats were excised, minced, and homogenized with a Teflon pestle in SHE buffer (250 mM sucrose, 10 mM HEPES, 1 mM EGTA, pH 7.3) *plus* 1 mM EDTA, 5 mM DTT, and 1 mM PMSF. Homogenates were centrifuged at 1,800*g* for 5 min at 4°C. The supernatants were recovered and centrifuged at 39,000*g* for 20 min at 4°C. Thereafter, the supernatants were concentrated to 1 ml with a centrifugal filter device (50,000 MWCO; Millipore, Billerica, MA) and mixed with 10% (v/v) glycerol and stored at −72°C until use for determination of enzyme activity.

CANCER BIOPSIES SAMPLING AND STORING

Human mammary carcinoma biopsies (200–300 μg) were collected by the "Tru-Cut" needle method [Maharaj and Pillay, 1991] from female patients of the Instituto Nacional de Cancerología, México, according to standardized and approved public health protocols. Fresh samples were immediately frozen in liquid N_2 until their use. For Western blot analysis, samples were washed, minced, and homogenized in 25 mM Tris–HCl, pH 7.6 *plus* 5 mM DTT, 1 mM EDTA, and 1 mM PMSF and centrifuged at 15,399*g* for 30 min at 4°C. The supernatant was collected and stored at −70°C until its use.

PFK-1 ACTIVITY

The reaction assay buffer was 10 mM $MgCl_2$, 0.15 mM NADH, 1.5 U aldolase, 2–3 U α-glycerophosphate dehydrogenase, 19–30 U trio-

sephosphate isomerase, 0.55–0.7 mM ATP, and 20 mM MOPS *plus* 20 mM imidazole, at the indicated pH, which was adjusted at 25°C with HCl or Tris. The reaction was carried out at 37°C, started by adding the cytosolic extract and following spectrophotometrically the NADH oxidation at 340 nm. The activity was determined under initial-rate conditions; and the absorbance baseline in the absence of one substrate was always subtracted. Controls were used to ensure that the reaction rate was a linear function of the following enzyme concentration ranges: 0.1–0.3, 0.09–0.2, 0.24–0.39, 0.2–0.6, and 0.06–0.15 mg protein in the absence of K^+; and 0.05–0.2, 0.08–0.2, 0.17–0.3, 0.13–0.4, and 0.06–0.13 mg protein in the presence of 140 mM K^+ for AS-30D, HeLa, MCF-7, rat liver, and rat heart, respectively. Kinetic parameters were calculated by non-linear global fitting of all experimental points to the indicated rate equation by using the Microcal Origin v. 5 software.

CALIBRATION OF METABOLITE STOCK SOLUTIONS

Stock solutions of Fru6P, ATP, AMP, Fru2,6BP, and citrate were routinely calibrated by using enzymatic standard protocols with hexose-phosphate isomerase (HPI) *plus* G6PDH, HK *plus* G6PDH, *Entamoeba histolytica* PPDK *plus* LDH, HPI *plus* G6PDH after alkaline hydrolysis, and citrate lyase *plus* malate dehydrogenase, respectively [Bergmeyer, 1974].

PFK-1 GENE SEQUENCING AND ISOFORM EXPRESSION

Total RNA was extracted from human HeLa and MCF7 carcinomas (5×10^6 cells, 80–90% confluency), rat hepatoma AS-30D (7×10^6 cells) or fresh rat liver or heart (30 mg tissue), with the RNeasy kit (Qiagen, Hilden, Germany). The cDNAs were obtained by reverse transcription with the SuperScript first-strand cDNA synthesis system (Invitrogen, Carlsbad, CA) using the oligo $(dT)_{12-18}$ primer. The PFK genes encoding for L, M, or C isoforms were amplified using the Phusion High Fidelity DNA polymerase (Finnzymes, Vantaa, Finland) and the oligonucleotides described in the Supplementary Table S1. After gel-purification, the PCR products were sequenced. This procedure was performed at least twice from independent biological samples to detect the presence of polymorphisms. For sequence alignments, the following mRNA sequences, deposited in the NCBI genes database, were used: for human isoforms, PFK-1M, NM_000289.5; PFK-1L, NM_002626.4; PFK-1C, NM_002627.4; and for rat isoforms, PFK-1L, NM_013190; PFK-1C, NM_206847.1, and PFK-1M BC094212.1.

WESTERN BLOT ANALYSIS

Tumor cells were suspended in 25 mM Tris–HCl buffer, pH 7.4, plus 0.5% Igepal NP40 and a protease inhibitor mixture (Calbiochem, San Diego, CA). Samples (40 μg) were separated under denaturating and reducing conditions by SDS–PAGE in 10% polyacrylamide gels. The proteins were blotted onto PVDF membranes (BioRad, Hercules, CA) and Western blot analysis was performed by immunoblotting with human anti-PFK-1M (1:1,000; Santa Cruz, CA), anti-PFK-L (1:500; Abcam, Cambridge, MA), anti-PFK-C (1:1000; Abcam), and anti-α-tubulin (1:1,000; Santa Cruz); although human antibodies were used, strong positive reaction with rodent samples were also observed. The hybridization bands were revealed with the corresponding secondary antibodies conjugated with horseradish peroxidase (Santa Cruz) and the ECL-plus detection system (Amersham, Buckinghamshire, UK). Densitometric analyses were performed using the Scion Image Software (Scion, Frederic, MD) and normalized against its respective load (α-tubulin) control, which corresponded to 100% intensity.

RESULTS

AS-30D HEPATOMA PFK-1 KINETICS

To correctly determine the V_m and K_m values of a cooperative enzyme, measurement of the rate at different substrate concentrations (and keeping constant the co-substrate ATP) should be carried out and, preferentially, also at different fixed concentrations of an allosteric modulator. Somewhat surprisingly, PFK-1 kinetics with Fru6P in the cytosolic fraction from AS-30D hepatoma at different Fru2,6BP, AMP, or K^+ concentrations showed a sigmoidal pattern of curves with different V_m values (Fig. 1). Fitting of this behavior to the concerted transition rate equation of Monod, Wyman, and Changeux for either exclusive or non-exclusive binding was poor. Similar deficient fitting was attained with the *V* allosteric system (similar substrate affinity and different catalytic constant by the two enzyme states) and with the mixed *K*–*V* system rate equations [Segel, 1975]. Finally, the rate equation that accurately predicted the AS-30D PFK-1 kinetic behavior was the exclusive ligand binding concerted transition model (e.g., the R enzyme state only binds the substrate and/or allosteric activator; the T state only binds the allosteric inhibitor) with non-essential hyperbolic activation (the R state can be further activated in a hyperbolic mixed-type fashion) (Fig. 2). The complete rate Equation (1) is described below.

The α and β parameters in this complex equation represent, respectively, the factors by which the ligand (e.g., substrate S, activator A) affinity (K_S, K_A) and catalytic capacity (V_m) are modified in the presence of an allosteric activator (see also Fig. 2). *L* is the allosteric transition constant defining the [T]o/[R]o ratio; and n is the number of interacting sites which is 4 for tetrameric PFK-1

$$v = V_m \left(\frac{1 + \frac{\beta A}{\alpha K_A}}{1 + \frac{A}{\alpha K_A}} \right) \left[\frac{\frac{S\left(1+\frac{A}{\alpha K_A}\right)}{K_S\left(1+\frac{A}{K_A}\right)} \left[1 + \frac{S\left(1+\frac{A}{\alpha K_A}\right)}{K_S\left(1+\frac{A}{K_A}\right)} \right]^{n-1}}{\frac{L}{\left(1+\frac{A}{K_A}\right)^n} + \left[1 + \frac{S\left(1+\frac{A}{\alpha K_A}\right)}{K_S\left(1+\frac{A}{K_A}\right)} \right]^n} \right] \quad (1)$$

Activation of PFK-1 from AS-30D hepatoma by Pi and NH_4^+ also fitted adequately with the rate Equation (1) (data not shown). The whole set of kinetic parameters, determined for the two substrates and five allosteric activators at pH values of 7.5 and 6.5, is shown in Table I. In addition, the AS-30D PFK-1 kinetics was evaluated under the physiological condition of high K^+, to elucidate whether the interaction with the different enzyme ligands is affected by the presence of this cation. It was observed that lowering pH from 7.5 to 6.5 promoted (i) a decrease in V_m which was non-significant; (ii) a decrease in Fru6P affinity (K_m increases); and (iii) an increase in the content of inactive enzyme (T) forms (e.g., *L* increased). In turn,

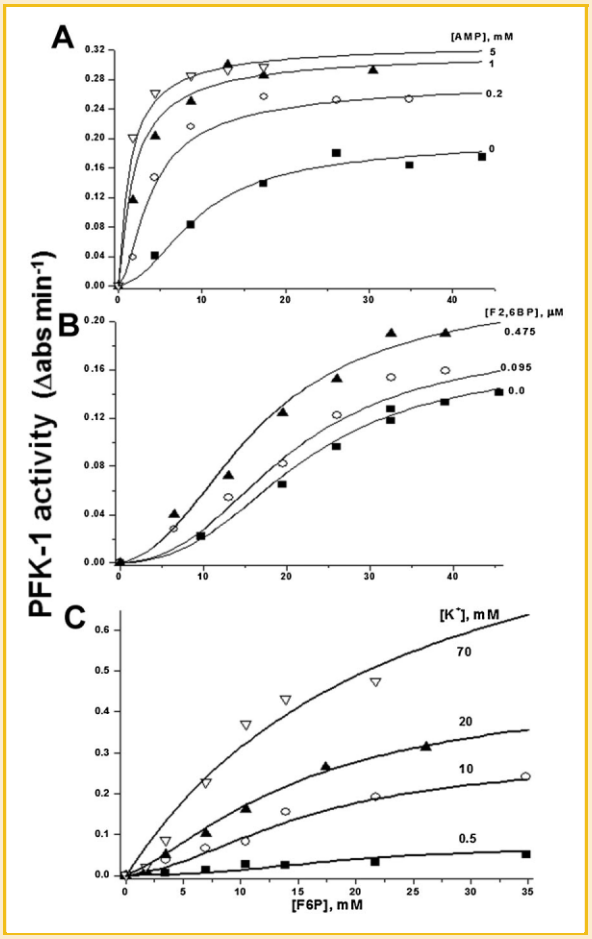

Fig. 1. Atypical kinetics of PFK-1 from AS-30D hepatoma cells. PFK-1 in the AS-30D cytosolic fraction was determined as described in the Materials and Methods Section at pH 7.5 and 37°C in a medium with no K^+ added, and with the indicated AMP (A), Fru2,6BP (B), or KCl (C) concentrations. The experimental points were globally fitted to Equation (1) by using the Microcal Origin v. 5 software. The values of the parameters for these particular experiments were for (A) $V_m = 72$ mU/mg protein (0.21 ΔAbs min^{-1} 0.235 mg^{-1}); $L = 12$; K_m Fru6P = 6.5 mM; $\alpha = 0.19$; $\beta = 1.58$; K_A AMP = 0.72 mM. B: V_m = 48.5 mU/mg protein (0.185 ΔAbs min^{-1} 0.306 mg^{-1}); $L = 59$; K_m Fru6P = 9.7 mM; $\alpha = 1.53$; $\beta = 2.7$; K_A Fru2,6BP = 1.14 μM. C: V_m = 56.25 mU/mg protein (0.079 ΔAbs min^{-1} 0.113 mg^{-1}); $L = 50$; K_m Fru6P = 8.6 mM; $\alpha = 4.5$; $\beta = 26$; K_A K^+ = 15.4 mM.

increasing K^+ prompted (i) a remarkable increase in V_m ($P < 0.005$ at pH 7.5); (ii) an increased affinity for Fru6P ($P < 0.01$ at pH 7.5); and (iii) an increased content of active enzyme (R) forms (Table I). On the other hand, hyperbolic kinetics for ATP (at saturating Fru6P and with or without saturating activator) was observed under all assayed conditions (Supplementary Fig. S1).

Regarding allosteric (and non-essential hyperbolic mixed-type) activators, it was determined that (i) lowering pH induced mixed effects either decreasing Fru2,6BP or increasing NH_4^+ and AMP affinity, or no effect on K^+ or Pi affinity; (ii) high K^+ did not modify affinity for Fru2,6BP and AMP, whereas it increased that for Pi (Table I). High K^+ also strongly blocked the activating effect by NH_4^+, whereas Fru2,6BP and AMP blocked each other for activation (data not shown). The strongest effect on increasing V_m (e.g., β value) was exerted by the two cation activators ($K^+ > NH_4^+ > Pi >> AMP$, Fru2,6BP), whereas the ligand affinity (e.g., α value) was slightly increased by AMP and Pi or markedly decreased by K^+, NH_4^+, and Fru2,6BP.

AS-30D PFK-1 kinetics in the presence of the allosteric inhibitors ATP or citrate showed sigmoidal behavior that fitted acceptably well the simple exclusive ligand binding concerted transition rate equation (Supplementary Fig. S1). The relatively high K_i (not IC_{50}) values here determined (Table I) prompted the evaluation of the AS-30D PFK-1 inhibitor sensitivity at fixed and low substrate concentrations, as usually determined by other authors that have reported lower IC_{50} values for both ATP [Sánchez-Martínez et al., 2000] and citrate [Staal et al., 1987]. The IC_{50} values for citrate and ATP at low (6.7 mM) Fru6P in K^+-based medium were, respectively, 0.78 and 0.96 mM at pH 6.5, and 5.8 and 1.02 mM at pH 7.5; these values can be lower at lower Fru6P but the rates attained were less reliable. In the presence of high, inhibitory (1.74 mM) ATP, the citrate IC_{50} values were 0.49 mM at pH 6.5 and 1.24 mM at pH 7.5. As a control, IC_{50} values for citrate of rat liver PFK-1 were also determined at low (5 mM) Fru6P, giving 4 and 1.8 mM in the absence and presence of inhibitory ATP (1.5 mM), respectively, in K^+-based medium at pH 7.5.

The relatively low affinity for citrate and ATP (high K_i values) also prompted the analysis of the H^+ concentration as a PFK-1 allosteric inhibitor. From the data shown in Table I it became evident that low pH induced a decrease in the affinities for Fru6P, Fru2,6BP, citrate and ATP (as allosteric inhibitor), and an increase in that for AMP. Due to the experimental variability of the different biological replicas used, the statistical significance of the lower V_m values at pH 6.5 versus pH 7.5 was not readily apparent. However, when V_m was determined at different pH values with the same experimental preparation (Fig. 3), potent inhibitory effect of high H^+ concentrations (>50 nM; pH range from 7.25 to 6.5) was clear under low or high K^+ and with or without activator. Similar V_m–pH curve profiles were attained with liver PFK-1 (data not shown).

PFK-1 KINETICS IN CERVICO-UTERINE HeLa AND BREAST MCF-7 CARCINOMAS

Kinetic analysis of PFK-1 from HeLa and MCF-7 carcinomas was also carried out but only at pH 7.5, due to the much lower cell yield. Enzyme behavior in the presence of Fru6P and any of the five allosteric activators was also well predicted by Equation (1). The data revealed that both human cancer PFK-1s have higher affinity for Fru6P, but their activities were 3.6- to 4.4-fold (HeLa) and 6- to 8-fold (MCF-7) lower (Table II), than AS-30D PFK-1. Affinities of both human cancer PFK-1s for Fru2,6BP and AMP (in the absence of K^+) were lower, and those for Pi (HeLa) and citrate (MCF-7) higher, than those of AS-30D PFK-1. High K^+ did not modify the affinity for Fru2,6BP, but it increased that for AMP, Pi, and ATP (as inhibitor) (Table II). The potency sequence for increasing V_m (β value) was Pi, $NH_4^+ > K^+ \geq$ Fru2,6BP, AMP. The MCF-7 PFK-1 showed the lowest K_m value for citrate and the highest for Fru2,6BP. These observations suggested the expression of different PFK-1 isoforms in AS-30D versus HeLa and MCF-7 cells.

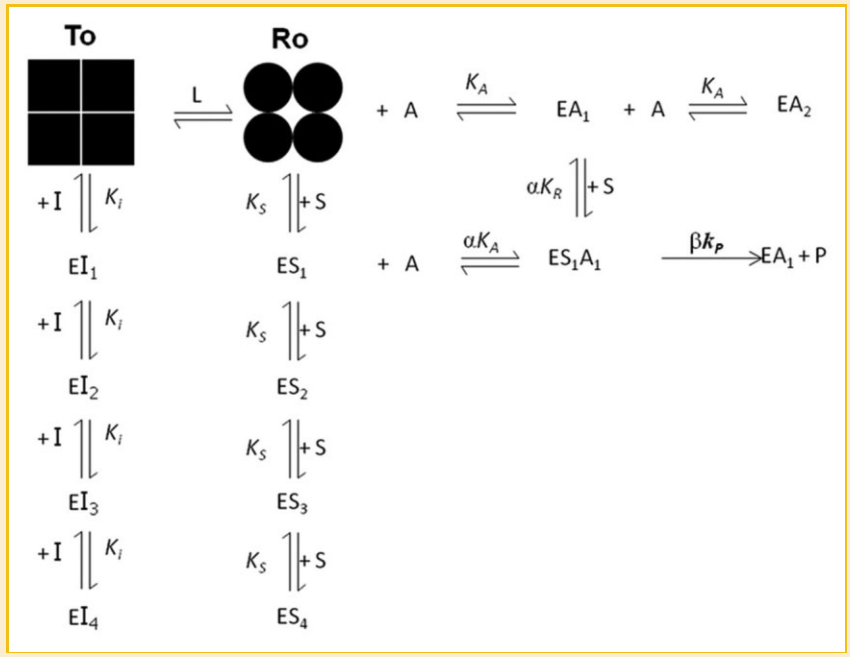

Fig. 2. Exclusive ligand binding concerted transition model with non-essential hyperbolic activation. The tetrameric squares represent the inactive T enzyme state, which is unable to bind or has very low affinity for the cooperative substrate S (*e.g.*, Fru6P) but has high affinity for allosteric inhibitors (*e.g.*, high ATP, citrate, H^+). The tetrameric circles represent the active R enzyme state, which may cooperatively bind the substrate and allosteric activators (*e.g.*, Fru2,6BP, AMP, Pi, K^+, NH_4^+). *L* represents the equilibrium constant for the enzyme state transition in the absence of ligands. The enzyme–substrate complexes ES_1, ES_2, ES_3, and ES_4 all catalyze the transformation of S to P at a rate equal to $k_p \times [ES]_n$, but for the sake of clarity this is not shown in the figure. In addition, the R state can be further activated by the same modulators in a non-essential hyperbolic mixed-type manner.

RAT LIVER AND HEART PFK-1 KINETICS

To elucidate whether the atypical kinetics of AS-30D, HeLa, and MCF-7 PFK-1s regarding activators was exclusive of tumor cells, kinetic analysis of PFK-1 from rat liver and heart was undertaken. However, rat liver and heart PFK-1 kinetics with Fru6P at different activator concentrations showed again a sigmoidal pattern of curves with different V_m values (Supplementary Fig. S2). In addition, lowering pH induced in rat liver PFK-1 (i) decreased V_m; and (ii) decreased Fru6P, Fru2,6BP, and NH_4^+ or increased K^+, and AMP affinities (Table III). In turn, increasing K^+ promoted in both liver and heart PFK-1, mainly at pH 7.5, (i) increased V_m ($P < 0.005$ at pH 7.5 in heart); and (ii) increased F6P or decreased Fru2,6BP affinities

TABLE I. AS-30D PFK-1 Substrate and Allosteric Ligand Kinetic Parameters

	No-K^+ medium		140 mM K^+ medium	
	pH 7.5	pH 6.5	pH 7.5	pH 6.5
V_m (nmol/min/mg protein)	77 ± 43 (14)	57 ± 18 (10)	250 ± 127 (21)	188 ± 98 (16)
K_m Fru6P (mM)	7 ± 2.3 (11)	13.3 ± 5.5 (11)	5 ± 2 (18)	8.3 ± 2.9 (16)
L ($[T]_0/[R]_0$)	22 ± 23 (11)	152 ± 15 (10)	18 ± 15 (18)	86 ± 53 (16)
K_m ATP (μM)	36.4 ± 6 (3)	29.2 (2)	43.6 ± 14 (4)	34 (2)
α_{NH_4+}	6.7 (2)	3.2		
β_{NH_4+}	13.7 (2)	5.8		
$K_{A\ NH_4+}$ (mM)	1.01 (2)	0.32		
α_{K^+}	3.7 (2)	3.6 (2)		
β_{K^+}	18.7 (2)	15.5 (2)		
KA_{K^+} (mM)	11.5 (2)	13.5 (2)		
$\alpha_{Fru2,6BP}$	1.75 ± 0.99 (3)	1.7 ± 1.6 (3)	4.4 ± 2.6 (3)	1.4 ± 0.9 (4)
$\beta_{Fru2,6BP}$	2.21 ± 0.47 (3)	2.06 ± 0.57 (3)	3.3 ± 2.2 (3)	2.3 ± 1.2 (4)
$K_{A,Fru2,6BP}$ (μM)	0.77 ± 0.51 (3)	8.3 ± 3.5 (3)	0.53 ± 0.4 (3)	15.9 ± 12 (4)
α_{AMP}	0.69 (2)	3.2 (2)	0.23 (2)	0.53 (2)
β_{AMP}	3.08 (2)	4.2 (2)	1.77 (2)	1.85 (2)
$K_{A,AMP}$ (mM)	0.73 (2)	0.15 (2)	0.86 (2)	0.28 (2)
α_{Pi}	0.96 (2)	0.78 (2)	0.44 (2)	2.8 (2)
β_{Pi}	16.6 (2)	8.3 (2)	4.6 (2)	3.3 (2)
$K_{A,Pi}$ (mM)	5.85 (2)	8.05 (2)	1.67 (2)	1.23 (2)
$K_{i,ATP}$ (mM)	1.82		1.75	2.5 (2)
$K_{i,citrate}$ (mM)	2.8	4.4	5.9 ± 1.7 (3)	17.2

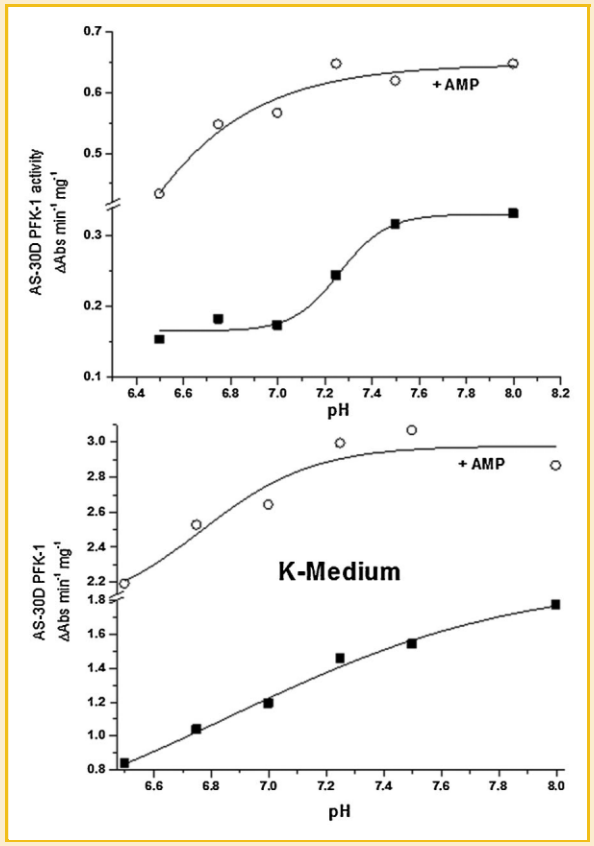

Fig. 3. Inhibitory effect of $[H^+]$ on maximal PFK-1 rate. AS-30D PFK-1 activity was determined under V_m conditions (saturating Fru6P) at the indicated pH values. In incubation media with no K^+ added the Fru6P concentrations used were 32–52 or 26–39 mM (+ AMP). In the 140 mM KCl medium, the Fru6P concentrations used were 19–39 or 13–26 mM (+ AMP). The protein concentrations used were 102–153 μg in no K^+-medium and 51–76 μg in 140 mM KCl medium.

($P < 0.005$ at pH 7.5 in heart; Tables III and IV). The heart PFK-1 showed the lowest K_m value for Fru6P and the highest for ATP (as substrate). The potency sequence for increasing V_m was $K^+ \geq NH_4^+ \geq Pi > Fru2,6BP$, AMP.

PFK-1 GENE SEQUENCE POLYMORPHISMS IN CANCER CELLS

To establish whether polymorphisms in the PFK-1 gene were present in cancer cells which might account for the differences in the enzyme activity, the nucleotide sequences of the three isoforms were determined for the five biological systems examined. PFK-1 mRNAs for the three isoforms were detected in human HeLa and MCF-7 cells (Supplementary Table S2). Translation of the obtained cDNA sequences evidenced the absence of amino acid changes in L and M isoforms from both carcinomas, although single nucleotide polymorphisms (SNPs) leading only to conserved amino acid changes were observed. Remarkably, the use of the oligonucleotide 5′-GCG CGC CAT ATG CAT AAA GAC GAG TTT CAT CTG AAA TTT TTC-3′ containing the first start codon (bold letters) of the long PFK-1M variant did not result in PCR amplification; therefore, only the short variant of this isoform was detected in both carcinomas (the start codon of which is located after 213 bases from the first ATG in the long variant PFK-1). In contrast, both human tumor PFK-1C nucleotide sequences showed several SNPs compared to the reported sequences from normal tissues, which resulted in conserved and non-conserved amino acid changes (Supplementary Table S2).

The rat PFK-1 mRNAs corresponding to the three isoforms were detected in liver, heart, and AS-30D hepatoma. Although SNPs were detected for the L and M isoforms all of them led to conservative amino acid changes. In contrast, non-conservative amino acid replacements were detected again only for the PFK-1C from AS-30D hepatoma (Supplementary Table S3).

PFK-1 ISOFORM IDENTIFICATION AND RELATIVE CONTENT

Analysis of the protein content by Western blotting of the PFK-1 isoforms revealed that rat liver and heart have predominantly the L

TABLE II. Human Tumor PFK-1 Substrate and Allosteric Ligand Kinetic Parameters

	HeLa cells (pH 7.5)		MCF-7 cells (pH 7.5)	
	No-K^+ medium	140 mM K^+ medium	No-K^+ medium	140 mM K^+ medium
V_m (nmol/min/mg protein)	21 ± 7 (17)	56 ± 23 (12)	13.1 ± 3.4 (12)	32.5 ± 10 (14)
K_m Fru6P (mM)	3.5 ± 0.9 (17)	1.1 ± 0.4 (11)	3.17 ± 0.82 (6)	1.03 ± 0.26 (10)
L ($[T]_0/[R]_0$)	29 ± 21 (13)	6.6 ± 5 (11)	112 ± 42 (6)	10 ± 9 (10)
K_m ATP (μM)	24.95 (2)	29.2 ± 1.5 (4)	68.9	67 ± 23 (4)
α_{NH_4+}	0.63 (2)		1.26 (2)	
β_{NH_4+}	2.73 (2)		3.65 (2)	
K_{A,NH_4+} (mM)	0.45 (2)		0.30 (2)	
α_{K^+}	0.25 ± 0.11 (3)		1.23 (2)	
β_{K^+}	1.05 ± 0.44 (3)		5.17 (2)	
KA_{K^+} (mM)	28 ± 19 (3)		24.1 (2)	
$\alpha_{Fru2,6BP}$	0.49 (2)	0.75 ± 0.4 (3)	2.0	0.31 ± 0.12 (3)
$\beta_{Fru2,6BP}$	1.38 (3)	1.18 ± 0.17 (3)	1.48	1.13 ± 0.25 (3)
$K_{A,Fru2,6BP}$ (μM)	1.0 (2)	0.99 ± 0.14 (3)	4.6	5.3 ± 4.6 (3)
α_{AMP}	0.91 ± 0.42	0.35 (2)	0.74	0.34 ± 0.26 (3)
β_{AMP}	0.61 ± 0.17	1.31 (2)	1.26	1.13 ± 0.23 (3)
$K_{A,AMP}$ (mM)	1.95 ± 3.1 (3)	0.9 (2)	5.8	0.78 ± 0.09 (3)
α_{Pi}	0.21 ± 0.18 (3)	0.58 (2)		0.49
β_{Pi}	1.69 ± 1.36 (3)	1.6 (2)		1.57
$K_{A,Pi}$ (mM)	4.52 ± 1.36 (3)	0.99 (2)		1.0
$K_{i,ATP}$ (mM)	>5.8	1.1		
$K_{i,citrate}$ (mM)	8.1 (2)	6.7 ± 3.8 (3)		0.49 ± 0.47 (3)

TABLE III. Liver PFK-1 Substrate and Allosteric Ligand Kinetic Parameters

	No-K^+ medium		140 mM K^+ medium	
	pH 7.5	pH 6.5	pH 7.5	pH 6.5
V_m (nmol/min/mg protein)	40.7 ± 25 (10)	16.4 ± 12.7 (3)	47 ± 29 (17)	32.5 ± 18 (11)
K_m Fru6P (mM)	4.9 ± 1.4 (10)	13.0 ± 5.2 (3)	3.0 ± 0.9 (10)	10.5 ± 2.1 (8)
L ($[T]_0/[R]_0$)	8.7 ± 7.3 (10)	23 ± 31 (3)	18.5 ± 15 (10)	8.3 ± 6.2 (8)
K_m ATP (μM)	72.9 (2)	35.2 (2)	39.5 ± 8 (4)	21.3 (2)
α_{NH_4+}	0.51 (2)	3.9		
β_{NH_4+}	2.4 (2)	3.0		
K_{A,NH_4+} (mM)	1.36 (2)	4.94		
α_{K^+}	2.1 (2)	3.1 (2)		
β_{K^+}	2.5 (2)	3.4 (2)		
KA_{K^+} (mM)	32.5 (2)	3.5 (2)		
$\alpha_{Fru2,6BP}$	1.2 (2)		0.91 ± 0.9 (3)	2.1 ± 0.5 (3)
$\beta_{Fru2,6BP}$	0.94 (2)		1.32 ± 0.4 (3)	4.2 ± 0.9 (3)
$K_{A,Fru2,6BP}$ (μM)	0.115 (2)		0.58 ± 0.3 (3)	4.1 ± 1.8 (3)
α_{AMP}	0.29 (2)		0.07	2.95 (2)
β_{AMP}	0.95 (2)		1.19	4.92 (2)
$K_{A,AMP}$ (mM)	1.63 (2)		1.55	0.10 (2)
α_{Pi}	0.64 (2)		0.13	3.23 (2)
β_{Pi}	1.21 (2)		1.12	3.7 (2)
$K_{A,Pi}$ (mM)	0.72 (2)		2.36	2.13 (2)
$K_{i,ATP}$ (mM)			2.9 (2)	2.5 (2)
$K_{i,citrate}$ (mM)			6.7 ± 4.3 (3)	18.9

and M isoforms, respectively, as previously documented [Vora et al., 1985b; Dunaway et al., 1988], whereas the L and M isoforms were expressed at apparently similar extents in AS-30D hepatocarcinoma. On the other hand, the C and M isoforms prevailed in cervicouterine HeLa and breast MCF-7 carcinomas, respectively (Fig. 4). No significant positive reactions for PFK-1L in heart, PFK-1M in liver, or PFK-1C in both heart and liver were detected indicating null experimental cross-reactivity of the respective antibodies; in turn, PFK-1C was only detected in HeLa cells and human platelets (data not shown). The relative HIF-1α content was also determined in an effort to establish whether this transcription factor has a preferred PFK-1 gene target. As expected, the three carcinomas showed increased HIF-1α contents versus liver and heart (Fig. 4), suggesting a correlation with the PFK-1 content but no with the expression of a particular PFK-1 isoform.

PFK-1 isoform protein content pattern of other human and rodent carcinomas was also analyzed (Fig. 5). Prostate PC-3 carcinoma expressed the three PFK-1 isoforms, colon HCT15 mainly expressed the M isoform, breast MDA-MB-231 and lung A549 carcinomas expressed both M and C, and no PFK-1 isoform was detected in lung SKLU, U87MG astrocytoma, and C6 glioma. Accordingly, M and L isoforms were detected, with only traces of PFK-1C, in both human breast biopsies from normal and tumorigenic tissues, with M isoform being the predominantly over-expressed isoform in cancerous tissue (Fig. 5).

TABLE IV. Heart PFK-1 Substrate and Allosteric Ligand Kinetic Parameters

	pH 7.5	
	No-K^+ medium	140 mM K^+ medium
V_m (nmol/min/mg protein)	152 ± 93 (8)	416 ± 211 (16)
K_m Fru6P (mM)	0.28 ± 0.22 (8)	0.145 ± 0.035 (11)
L ($[T]_0/[R]_0$)	25 ± 16 (8)	18 ± 8 (11)
K_m ATP (μM)	88.5	74 ± 13 (3)
α_{NH_4+}	1.04	
β_{NH4+}	2.86	
K_{A,NH_4+} (mM)	0.90	
α_{K^+}	5.0 (2)	
β_{K^+}	13 (2)	
KA_{K^+} (mM)	16.6 (2)	
$\alpha_{F2,6BP}$	0.87 (2)	2.32 ± 0.33 (3)
$\beta_{F2,6BP}$	1.17 (2)	1.52 ± 0.35 (3)
$K_{A,F2,6BP}$ (μM)	1.24 (2)	3.5 ± 0.2 (3)
α_{AMP}	0.5	1.67 (2)
β_{AMP}	0.36	0.65 (2)
$K_{A,AMP}$ (mM)	0.05	1.13 (2)
α_{Pi}	0.37	1.63 (2)
β_{Pi}	4.4	1.37 (2)
$K_{A,Pi}$ (mM)	7.2	3.46 (2)
$K_{i,ATP}$ (mM)		25
$K_{i,citrate}$ (mM)	0.146	0.64 ± 0.19 (3)

DISCUSSION

PROS AND CONS OF KINETIC ANALYSIS IN CELLULAR EXTRACTS

Enzyme kinetics is usually carried out with isolated proteins from either native sources or over-expressing bacterial strains. This approach avoids interference by contaminating enzyme activities. However, only the determination of enzyme activities in cellular extracts can provide the physiological relevant V_m ($= k_{cat} \times [E]_t$) and V_m/K_m ratio (catalytic efficiency) values, which allows for an appropriate comparison with other activities for metabolic pathway reconstitution and/or modeling purposes. This is especially important for cells simultaneously expressing several iso-enzymes, as well as for enzymes able to form heteromeric states such as PFK-1. In addition, the presence of other proteins in cellular extracts does not affect the binding kinetic parameters as the differences in concentration between ligands (μM, mM) and proteins (pM, nM) are of several orders of magnitude.

For the present study, special care was taken to always determine activities in the protein concentration–enzyme activity linear range. Thus, the flux rate of the mini-pathway built to determine PFK-1 activity (PFK-1→ALDO→TPI→α-GPDH) was exclusively controlled by the PFK-1 added. The non-dialyzed cell-free extracts are certainly

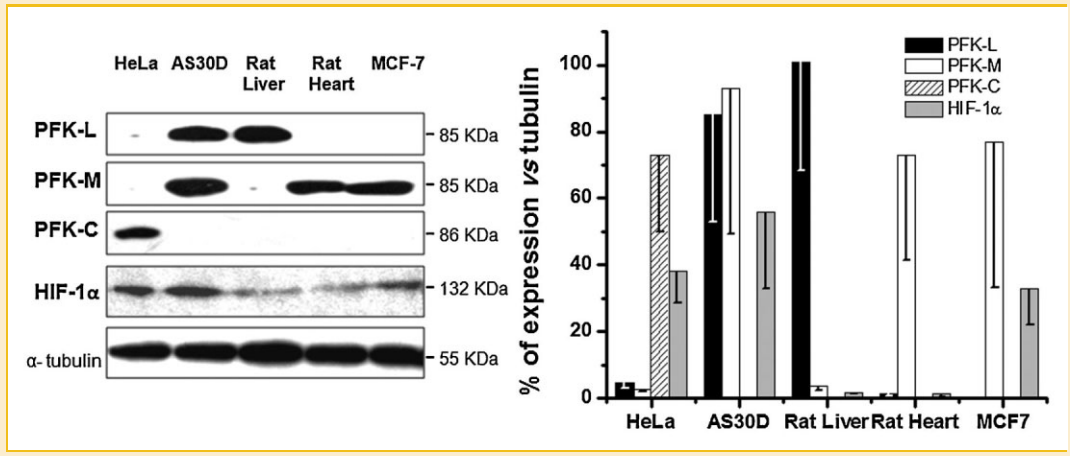

Fig. 4. Expression and relative content of PFK-1 isoforms and HIF-1α in cancer and normal cells. Data represent the mean ± SD of at least three independent preparations.

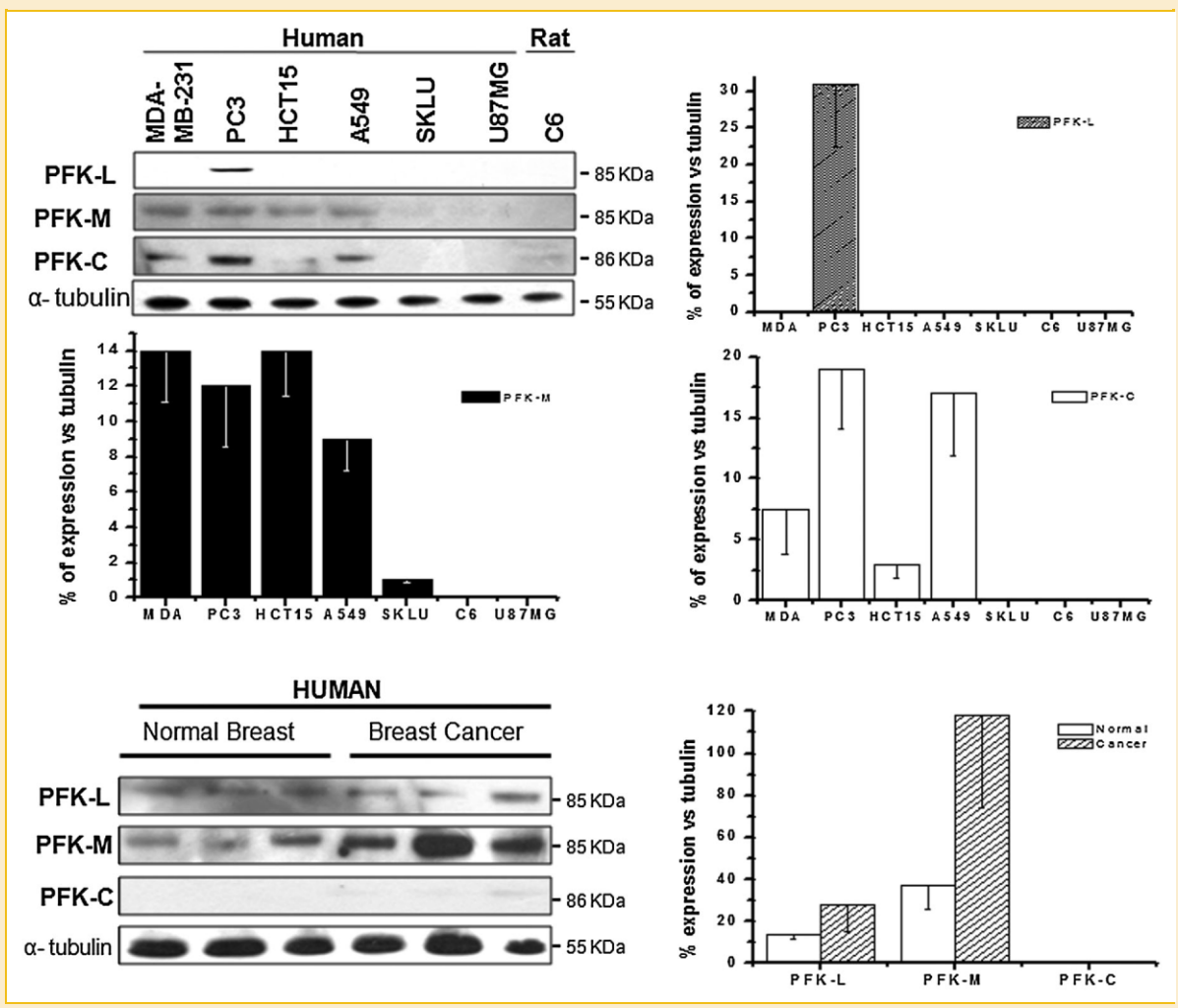

Fig. 5. Expression and relative content of PFK-1 isoforms in different human and rodent carcinomas. Data represent the mean ± SD of at least three independent preparations.

not-well defined systems, which might affect the reproducibility of the kinetic data. However, the allosteric modulators of PFK-1, assayed in the present study, are not of the tightly-bound type and therefore they rapidly equilibrate with the medium. The dilution factors at which the cytosolic fractions were assayed for PFK-1 activity were extremely high (>500 for liver and >1,000 for all other preparations) avoiding the presence of contaminating ligand concentrations. Therefore, the PFK-1 activity here determined was responsive only to the added substrates and modulators.

The main problem to obtain accurate kinetic parameters in cellular extracts may be the presence of competing activities. For instance, the presence of contaminating ATPase or HPI activities may thwart assay reliability of PFK-1 activity in cellular extracts. In the present study, this problem was circumvented by starting the reaction with the addition of the cytosolic fraction (*e.g.*, by not preincubating the cellular extract with the added ATP before starting the reaction) and by adding excess of coupling enzymes to favorably compete with contaminating activities. Indeed, reliable and reproducible PFK-1 activities were achieved at low ATP concentrations (15–100 μM) in all the cytosolic fractions assayed. However, care has to be taken when higher cytosolic protein concentrations are used because the activity of the PFK-1 and coupling enzymes may be over-passed by the increased contaminating enzymes.

Furthermore, to generate physiological relevant kinetic parameters, all assays were carried out at 37°C, contrasting with most other studies done at lower, non-physiological temperatures (25, 30°C). To correctly apply the rate-equations, only initial rates were considered; however, in some conditions (*i.e.*, high Fru6P and activator concentrations) the initial rate slowly increased along the reaction time, although this secondary rate was not taken into account for calculations. This hysteretic behavior of PFK-1 has been documented for its interaction (M > C > L) with α-tubulin and the cytoskeleton leading to inactivation [Lehotzky et al., 1993; Vertessy et al., 1996].

Actual affinity constants (K_m, K_A, K_i) instead of meaningless and condition-dependent constant ($K_{0.5}$, IC_{50}) values were determined in the present work under a variety of near-physiological conditions, by using complex rate equations and making the adequate experiments of varying substrate concentration at different fixed allosteric modulator concentrations.

PHYSIOLOGICAL RELEVANCE OF PFK-1 KINETIC DATA

Analysis of the PFK-1 expression pattern in human and rat cancer cells has shown a prevalence of the L or C isoforms over the M isoform [Vora et al., 1985a; Oskam et al., 1985; Staal et al., 1987; Sánchez-Martínez and Aragón, 1997]. The detailed systematic kinetic analysis of the present work in turn shows that to achieve both increased flux through the glycolytic pathway (for ATP and H^+ production) and higher levels of intermediary metabolites (for biosyntheses), over-expression of PFK-1L and/or PFK-1C over PFK-1M should be favored because these isoforms have lower affinity for Fru6P (avoiding saturation at high Fru6P) and citrate (avoiding allosteric inhibition), and higher affinity for allosteric activators (ensuring full activity). The PFK-1M isoform certainly shows the highest affinity for Fru6P and the highest V_m, but it also shows the highest affinity for the inhibitor citrate and the lowest affinity for the activator Fru2,6BP, suggesting low activity under high Krebs cycle and mitochondrial activity (which produce citrate).

In fact, AS-30D hepatoma, which expresses PFK-1L ≥ PFK-1M, and cervico-uterine HeLa carcinoma, which expresses PFK-1C, develop relatively high aerobic glycolytic rates of 21 and 16 nmol lactate min^{-1} mg $protein^{-1}$ and high levels of glycolytic intermediaries (4–200 times vs. rat liver or hepatocytes) and activators (1.5–25 times vs. rat liver or hepatocytes) [Marín-Hernández et al., 2006, 2011]. In contrast, breast MCF-7 carcinoma, which expresses PFK-1M, maintains a low glycolytic rate of 2.2 nmol min^{-1} mg $protein^{-1}$, which is similar to the aerobic glycolytic flux reported for the heart of 1.2 nmol min^{-1} mg $protein^{-1}$, which also expresses predominantly PFK-1M [Nascimben et al., 2004; see also Fig. 4]. Indeed, the PFK-1 activity, predicted by Equation (1) in the presence of physiological concentrations of Fru6P, Fru2,6BP and citrate, correlated well with the glycolytic fluxes (Supplementary Fig. S3; see legend to this figure for metabolite concentration values). PC3 prostate carcinoma (PFK-1L > PFK-1C = PFK-1M) also exhibits high glycolytic rates of 16 nmol min^{-1} mg $protein^{-1}$, but metabolite concentrations for this cancer are not available.

Exceptions to the pattern of PFK-1L or PFK-1C/high glycolysis, and PFK-1M/low glycolysis (Supplementary Fig. S3) exist. Liver or isolated hepatocytes exhibit low glycolytic rate of 2 nmol min^{-1} mg $protein^{-1}$ [Marín-Hernández et al., 2006], but they predominantly express PFK-1L [Oskam et al., 1985; Vora et al., 1985b; see also Fig. 4], whereas HTC-15 colon and MDA-MB-23 breast carcinomas have glycolytic rates of 20 and 17 nmol min^{-1} mg $protein^{-1}$, but they expressed PFK-1M ≥ PFK-1C (Fig. 5). These last observations suggest that PFK-1L, although fully activated by Fru2,6BP (K_A of 0.5 μM, [F2,6BP] of 4.5 μM), is expressed at a relatively low content in liver, and that PFK-1M expressed in some human carcinomas appears to be inactive or that the C isoform activity predominates. Furthermore, it is also necessary to consider that the glycolytic flux is controlled by several steps (glucose transport, HK, HPI) and not only by PFK-1 activity [Marín-Hernández et al., 2006, 2011]. Therefore, a strict relationship between PFK-1 isoform content and activity with the glycolytic flux cannot be expected for all cancers.

HIF-1α, the key transcriptional factor that is over-expressed in cancer cells (see Fig. 4) and induces enhanced glycolytic capacity and angiogenesis (reviewed in Marín-Hernández et al., 2009), regulates PFK-1 expression. It has been documented that HIF-1α up-regulates the transcription of the PFK-1L isoform [Semenza et al., 1994; Rankin and Giaccia, 2008]. However, the other PFK-1 isoforms may also be HIF-1α target genes. Putative HIF-1α binding sites in the promoter regions are found in the human and mouse PFK-1C genes; moreover, the PFK-1M and PFK-1C mRNA levels are increased by hypoxia and HIF-1α in human muscle and skin fibroblasts [Moeller et al., 2005; Vogt et al., 2001].

The analysis of the human PFK-1 gene sequences deposited in Gene Bank (PFK-1M: NG_016199; PFK-1L: NC_000021; PFK-1C: NC_000010) revealed that there are 10 (M), 10 (L) and 14 (C) possible binding sites (TACGTG or TAGGTG) for HIF-1α in the 5′ untranslated region at 5,000 bp distance, and 3 (M), 6 (L) and 2

(C) sites at 1,500 bp distance, from the start codon. Moreover, HIF-1α was high in human HeLa and MCF-7 cancer cells (*cf.* Fig. 4) in which only the PFK-1C and PFK-1M isoforms, respectively, were expressed. In preliminary experiments, both human cancer cell lines subjected to hypoxia showed increased HIF-1α levels together with increased protein content of the three PFK-1 isoforms. Therefore, it appears that HIF-1α transcriptional activity has not a preferred target within the PFK-1 genes.

In non-tumor cells, PFK-1 is involved in the Pasteur effect through its presumed inhibition by citrate, and perhaps high ATP, induced by the O_2-dependent increase in the Krebs cycle and oxidative phosphorylation fluxes [Barker et al., 1966; Eigenbrodt and Glossmann, 1980]. Although the H^+ was the most potent PFK-1 allosteric inhibitor, cytosolic pH is not lowered by glycolysis in normal cells. The PFK-1L K_i values determined for citrate and ATP were relatively high (see Table III) making difficult to visualize an effective PFK-1 inhibition in liver and AS-30D hepatoma. However, at non-saturating Fru6P and in the absence of activators, low citrate or ATP (<1 mM) may potently block PFK-1 activity in the liver, that is, IC_{50} values ~1 mM. Moreover, PFK-1 activity in the heart, predicted by Equation (1) in the presence of physiological concentrations of Fru6P (80 μM) and Fru2,6BP (0.78 μM) [Zorzano et al., 1985; Nascimben et al., 2004], can be fully abolished by physiological concentrations of citrate (2.5 mM), or ATP (9.8 mM; Nascimben et al., 2004), or of both inhibitors.

Due to the enhanced glycolytic activity in cancer cells resulting in over-production of lactate + H^+, both the cytosol and the extracellular milieu become acidified [Rodríguez-Enríquez et al., 2001; Gerweck et al., 2006]. In addition, higher cytosolic ATP and citrate concentrations are also found in cancer cells, and citrate was also a potent inhibitor of MCF-7 PFK-1 (*cf.* Table II). The enhanced levels of the three PFK-1 allosteric inhibitors should lead to a stronger Pasteur effect in cancer cells. In consequence, if the activator levels in MCF-7 cells are relatively low, then the Pasteur effect may also surge in this carcinoma.

In turn, AS-30D and other cancer cells over-express PFK-1L, the least sensitive isoform to citrate, and establish high levels of the activators Fru2,6BP and AMP [Loiseau et al., 1985; Mojena et al., 1985; Denis et al., 1986; Nissler et al., 1995; Marín-Hernández et al., 2006, 2011] to overcome the citrate, ATP and H^+ inhibitory effect, ensuring high PFK-1 activity [Meldolesi et al., 1976; Van Schaftingen et al., 1981; Marín-Hernández et al., 2006] and leading to glycolysis insensitivity towards O_2 (e.g., lack of Pasteur effect in most cancer cells). Thus, assuming that PFK-1 fully mediates the Pasteur Effect and by modeling the PFK-1 activity with the kinetic parameters here determined, a complete mechanistic understanding of the onset of this cellular process, or its absence, in normal and tumor cells can be readily reached.

In addition, a fully activated and highly over-expressed PFK-1 [Nakashima et al., 1988; Stubbs et al., 2003; Marín-Hernández et al., 2006] confers no glycolytic flux-limitation and exerts negligible flux control [Marín-Hernández et al., 2006, 2011]. Perhaps, in tumors with low PFK-1 expression [Shonk et al., 1965; Colomer et al., 1987] and/or low levels of Fru2,6BP [Colomer et al., 1987; Clem et al., 2008] and AMP [Traut, 1994; Marín-Hernández et al., 2011], significant flux-control by PFK-1 might be achieved.

NUCLEOTIDE POLYMORPHISMS IN THE PFK-1 GENE ISOFORMS

The analysis of the PFK-1 mRNA sequences from the cells here analyzed indicated the presence of SNPs that resulted in non-conservative amino acid replacements only in the C isoform gene. Therefore, the differences in the kinetic properties of the L or M isoforms between tumor and normal PFK-1 cannot be attributed to nucleotide sequence changes. As the C isoform protein is not significantly expressed in AS-30D and MCF-7 cells, the effect of the SNPs on the enzyme activity is therefore silent in these carcinomas. On the other hand, HeLa cells mainly express the PFK-1C isoform containing the amino acid replacement D339N. This substitution is located in the linker that connects the α-helix 12 with the β-strand K, which is far from the known active and regulatory sites [Banaszak et al., 2011]. Thus, it appears unlikely that this replacement may affect the structure or kinetic properties of the HeLa PFK-1C.

PFK-1 ISOFORM KINETIC SIGNATURE

Among the numerous kinetic parameters determined here, only a few of them were useful for providing a clear kinetic signature for each isoform. Thus, PFK-1M (heart, MCF-7) was the isoform with the most distinguishable ligand affinity values for Fru6P, ATP (as substrate), Fru2,6BP, and citrate. The sequence of these kinetic parameters for the three isoforms was as follows (at pH 7.5 in K-based medium; Tables I–IV; Supplementary Figs. S1 and S2):

K_m F6P: PFK-M ≤ PFK-C < PFK-L
($P < 0.005$ for heart vs. MCF-7, HeLa or liver; $P < 0.005$ for liver vs. MCF-7 or AS-30D; Student's *t*-test for non-paired samples);
K_m ATP: PFK-C ≤ PFK-L < PFK-M
($P < 0.05$ for HeLa vs. liver, heart or MCF-7; $P < 0.05$ for liver or AS-30D vs. heart);
K_A FBP: PFK-L < PFK-C < PFK-M
($P < 0.005$ for heart vs. HeLa, liver or AS-30D);
K_i citrate: PFK-M < PFK-L < PFK-C
($P < 0.01$ for heart or MCF-7 vs. AS-30D; $P < 0.05$ for heart or MCF-7 vs. HeLa)

in which PFK-1M activity was only present in the heart and MCF-7 cells, PFK-1L activity was only found in the liver, and PFK-1C activity was exclusively developed in HeLa cells (see Fig. 4).

In turn, at pH 7.5 and high K^+ the K_m for ATP of AS-30D PFK-1 which contains both L and M isoforms was 43.6 μM (Table I) while that for liver enzyme (L form) was 39.5 μM (Table III) and heart form (M type) was 74 μM (Table IV). Similarly, the K_A for Fru2,6BP of AS-30D PFK-1 was 0.53 μM, while that for liver was 0.58 μM and for M isoform was 3.5 μM. The K_i for citrate of AS-30D PFK-1 was 5.9 mM, while those for liver and heart were 6.7 and 0.6 mM, respectively. And the K_m for Fru6P of AS-30D PFK-1 was 5 mM, while that for liver was 3 mM and for M isoform was 0.14 mM. Based on this kinetic profile, it became apparent that PFK-1L predominated over the M isoform for activity in the AS-30D cells. In turn, the differences in V_m among the five biological systems assayed ($P < 0.005$ for heart versus AS-30D, HeLa, liver, MCF-7; $P < 0.005$ for HeLa versus AS-30D or MCF-7) reflected differences in gene expression, and transcriptional and translational processes.

In conclusion, these four affinity values can be reliably used as a kinetic signature for further PFK-1 isoform identification in other tissues. These observations emphasize that not only changes in mRNA, protein content, or even enzyme activity, suffice to draw conclusions about how glycolysis can be controlled in tumor cells. It is also necessary to analyze how the activity of key (*e.g.*, controlling) pathway enzymes such as PFK-1 is further regulated through changes in the concentrations of pathway intermediary metabolites and modulators.

ACKNOWLEDGMENTS

The present work was partially supported by grants from CONACyT-México (nos. 80534, 123636, 83084, 106583, 107183) and Instituto de Ciencia y Tecnología del Distrito Federal (no. PICS08-5).

REFERENCES

Banaszak K, Mechin I, Obmolova G, Oldham M, Chang SH, Ruiz T, Radermacher M, Kopperschlager G, Rypniewski W. 2011. The crystal structures of eukaryotic phosphofructokinases from baker's yeast and rabbit skeletal muscle. J Mol Biol 407:284–297.

Barker J, Khan MA, Solomos T. 1966. Mechanism of the Pasteur effect. Nature 211:547–548.

Bergmeyer HU. 1974. Methods of enzymatic analysis, 1st edition. Weinheim: Verlag Chemie.

Clem B, Telang S, Clem A, Yalcin A, Meier J, Simmons A, Rasku MA, Arumugam S, Dean WL, Eaton J, Lane A, Trent JO, Chesney J. 2008. Small-molecule inhibition of 6-phosphofructo-2-kinase activity suppresses glycolytic flux and tumor growth. Mol Cancer Ther 7:110–120.

Colomer D, Vives-Corrons JL, Pujades A, Bartrons R. 1987. Control of phosphofructokinase by fructose 2,6-bisphosphate in B-lymphocytes and B-chronic lymphocytic leukemia cells. Cancer Res 47:1859–1862.

Denis C, Paris H, Murat JC. 1986. Hormonal control of fructose 2,6-bisphosphate concentration in the HT29 human colon adenocarcinoma cell line. Alpha 2-adrenergic agonists counteract effect of vasoactive intestinal peptide. Biochem J 239:531–536.

dos Santos MA, Borges JB, de Almeida DC, Curi R. 2004. Metabolism of the microregions of human breast cancer. Cancer Lett 216:243–248.

Dunaway GA, Kasten TP, Sebo T, Trapp R. 1988. Analysis of the phosphofructokinase subunits and isoenzymes in human tissues. Biochem J 251:677–683.

Eigenbrodt E, Glossmann H. 1980. Glycolysis: one of the keys to cancer? Trends Pharmacol Sci 1:240–245.

El-Bacha T, de Freitas MS, Sola-Penna M. 2003. Cellular distribution of phosphofructokinase activity and implications to metabolic regulation in human breast cancer. Mol Genet Metab 79:294–299.

Gerweck LE, Vijayappa S, Kozin S. 2006. Tumor pH controls the in vivo efficacy of weak acid and base chemotherapeutics. Mol Cancer Ther 5:1275–1279.

Jannaschk D, Burgos M, Centerlles JJ, Ovadi J, Cascante M. 1999. Application of metabolic control analysis to the study of toxic effects of copper in muscle glycolysis. FEBS Lett 445:144–148.

Kashiwaya Y, Sato K, Tsuchiya N, Thomas S, Fell DA, Veech RL, Passonneau JV. 1994. Control of glucose utilization in working perfused rat heart. J Biol Chem 269:25502–25514.

Koster JF, Slee RG, Van Berkel TJ. 1980. Isoenzymes of human phosphofructokinase. Clin Chim Acta 103:169–173.

Lehotzky A, Telegdi M, Liliom K, Ovadi J. 1993. Interaction of phosphofructokinase with tubulin and microtubules. Quantitative evaluation of the mutual effects. J Biol Chem 268:10888–10894.

Loiseau AM, Rousseau GG, Hue L. 1985. Fructose 2,6-bisphosphate and the control of glycolysis by glucocorticoids and by other agents in rat hepatoma cells. Cancer Res 45:4263–4269.

López-Gómez FJ, Torres-Márquez ME, Moreno-Sánchez R. 1993. Control of oxidative phosphorylation in AS-30D hepatoma mitochondria. Int J Biochem 25:373–377.

Maharaj B, Pillay S. 1991. "Tru-Cut" needle biopsy of the liver: importance of the correct technique. Postgrad Med J 67:170–173.

Marín-Hernández A, Rodríguez-Enríquez S, Vital-González PA, Flores-Rodríguez FL, Macias-Silva M, Sosa-Garrocho M, Moreno-Sánchez R. 2006. Determining and understanding the control of glycolysis in fast-growth tumor cells. Flux control by an over-expressed but strongly product-inhibited hexokinase. FEBS J 273:1975–1988.

Marín-Hernández A, Gallardo-Perez JC, Ralph SJ, Rodríguez-Enríquez S, Moreno-Sánchez R. 2009. HIF-1alpha modulates energy metabolism in cancer cells by inducing over-expression of specific glycolytic isoforms. Mini Rev Med Chem 9:1084–1101.

Marín-Hernández A, Gallardo-Perez JC, Rodríguez-Enríquez S, Encalada R, Moreno-Sánchez R, Saavedra E. 2011. Modeling cancer glycolysis. Biochim Biophys Acta 1807:755–767.

Meldolesi MF, Macchia V, Laccetti P. 1976. Differences in phosphofructokinase regulation in normal and tumor rat thyroid cells. J Biol Chem 251:6244–6251.

Moeller LC, Dumitrescu AM, Refetoff S. 2005. Cytosolic action of thyroid hormone leads to induction of hypoxia-inducible factor-1alpha and gycolytic genes. Mol Endocrinol 19:2955–2963.

Mojena M, Bosca L, Hue L. 1985. Effect of glutamine on fructose 2,6-bisphosphate and on glucose metabolism in HeLa cells and in chick-embryo fibroblasts. Biochem J 232:521–527.

Moreno-Sánchez R, Rodríguez-Enríquez S, Marín-Hernández A, Saavedra E. 2007. Energy metabolism in tumor cells. FEBS J 274:1393–1418.

Moreno-Sánchez R, Rodríguez-Enríquez S, Saavedra E, Marín-Hernández A, Gallardo-Pérez JC. 2009. 2009The bioenergetics of cancer: is glycolysis the main ATP supplier in all tumor cells? Biofactors 35:209–225.

Nakashima RA, Paggi MG, Scott LJ, Pedersen PL. 1988. Purification and characterization of a bindable form of mitochondrial bound hexokinase from the highly glycolytic AS-30D rat hepatoma cell line. Cancer Res 48:913–919.

Nascimben L, Ingwall JS, Lorell BH, Pinz I, Schultz V, Tornheim K, Tian R. 2004. Mechanisms for increased glycolysis in the hypertrophied rat heart. Hypertension 44:662–667.

Nissler K, Petermann H, Wenz I, Brox D. 1995. Fructose 2,6-bisphosphate metabolism in Ehrlich ascites tumour cells. J Cancer Res Clin Oncol 121:739–745.

Oskam R, Rijksen G, Staal GE, Vora S. 1985. Isozymic composition and regulatory properties of phosphofructokinase from well-differentiated and anaplastic medullary thyroid carcinomas of the rat. Cancer Res 45:135–142.

Rankin EB, Giaccia AJ. 2008. The role of hypoxia-inducible factors in tumorigenesis. Cell Death Differ 15:678–685.

Rapoport TA, Heinrich R, Jacobasch G, Rapoport S. 1974. A linear steady-state treatment of enzymatic chains. A mathematical model of glycolysis of human erythrocytes. Eur J Biochem 42:107–120.

Rodríguez-Enríquez S, Juarez O, Rodríguez-Zavala JS, Moreno-Sánchez R. 2001. Multisite control of the Crabtree effect in ascites hepatoma cells. Eur J Biochem 268:2512–2519.

Saavedra E, Encalada R, Pineda E, Jasso-Chávez R, Moreno-Sánchez R. 2005. Glycolysis in *Entamoeba histolytica*. Biochemical characterization of recombinant glycolytic enzymes and flux control analysis. FEBS J 272:1767–1783.

Sánchez-Martínez C, Aragón JJ. 1997. Analysis of phosphofructokinase subunits and isozymes in ascites tumor cells and its original tissue, murine mammary gland. FEBS Lett 409:86–90.

Sánchez-Martínez C, Estevez AM, Aragón JJ. 2000. Phosphofructokinase C isozyme from ascites tumor cells: cloning, expression, and properties. Biochem Biophys Res Commun 271:635–640.

Segel IH. 1975. Enzyme kinetics, 1st edition. New York: Wiley.

Semenza GL, Roth PH, Fang HM, Wang GL. 1994. Transcriptional regulation of genes encoding glycolytic enzymes by hypoxia-inducible factor 1. J Biol Chem 269:23757–23763.

Shonk CE, Arison RN, Koven BJ, Majima H, Boxer GE. 1965. Enzyme patterns in human tissues. 3. Glycolytic enzymes in normal and malignant tissues of the colon and rectum. Cancer Res 25:206–213.

Staal GE, Kalff A, Heesbeen EC, van Veelen CW, Rijksen G. 1987. Subunit composition, regulatory properties, and phosphorylation of phosphofructokinase from human gliomas. Cancer Res 47:5047–5051.

Stubbs M, Bashford CL, Griffiths JR. 2003. Understanding the tumor metabolic phenotype in the genomic era. Curr Mol Med 3:49–59.

Torres NV, Mateo F, Melendez-Hevia E, Kacser H. 1986. Kinetics of metabolic pathways. A system in vitro to study the control of flux. Biochem J 234:169–174.

Traut TW. 1994. Physiological concentrations of purines and pyrimidines. Mol Cell Biochem 140:1–22.

Van Schaftingen E, Jett MF, Hue L, Hers HG. 1981. Control of liver 6-phosphofructokinase by fructose 2,6-bisphosphate and other effectors. Proc Natl Acad Sci USA 78:3483–3486.

Vertessy BG, Kovacs J, Ovadi J. 1996. Specific characteristics of phosphofructokinase-microtubule interaction. FEBS Lett 379:191–195.

Vogt M, Puntschart A, Geiser J, Zuleger C, Billeter R, Hoppeler H. 2001. Molecular adaptations in human skeletal muscle to endurance training under stimulated hypoxic conditions. J Appl Physiol 91:173–182.

Vora S, Halper JP, Knowles DM. 1985a. Alterations in the activity and isozymic profile of human phosphofructokinase during malignant transformation in vivo and in vitro: transformation- and progression-linked discriminants of malignancy. Cancer Res 45:2993–3001.

Vora S, Oskam R, Staal GE. 1985b. Isoenzymes of phosphofructokinase in the rat. Demonstration of the three non-identical subunits by biochemical, immunochemical and kinetic studies. Biochem J 229:333–341.

Zorzano A, Balon TW, Brady LJ, Rivera P, Garetto LP, Young JC, Goodman MN, Ruderman NB. 1985. Effects of starvation and exercise on concentrations of citrate, hexose phosphates and glycogen in skeletal muscle and heart. Evidence for selective operation of the glucose-fatty acid cycle. Biochem J 232:585–591.